NASA/TM–2020-5003145

# Progressive Failure Analysis Correlation with Notched Composite Laminate Test Data

*Arunkumar Satyanarayana and Sandra P. Walker*
*Langley Research Center, Hampton, Virginia*

*Kevin E. Gould*
*Analytical Mechanics Associates, Inc., Hampton, Virginia*

National Aeronautics and
Space Administration

Langley Research Center
Hampton, Virginia 23681-2199

June 2020

## NASA STI Program . . . in Profile

Since its founding, NASA has been dedicated to the advancement of aeronautics and space science. The NASA scientific and technical information (STI) program plays a key part in helping NASA maintain this important role.

The NASA STI program operates under the auspices of the Agency Chief Information Officer. It collects, organizes, provides for archiving, and disseminates NASA's STI. The NASA STI program provides access to the NTRS Registered and its public interface, the NASA Technical Reports Server, thus providing one of the largest collections of aeronautical and space science STI in the world. Results are published in both non-NASA channels and by NASA in the NASA STI Report Series, which includes the following report types:

- TECHNICAL PUBLICATION. Reports of completed research or a major significant phase of research that present the results of NASA Programs and include extensive data or theoretical analysis. Includes compilations of significant scientific and technical data and information deemed to be of continuing reference value. NASA counter-part of peer-reviewed formal professional papers but has less stringent limitations on manuscript length and extent of graphic presentations.

- TECHNICAL MEMORANDUM. Scientific and technical findings that are preliminary or of specialized interest, e.g., quick release reports, working papers, and bibliographies that contain minimal annotation. Does not contain extensive analysis.

- CONTRACTOR REPORT. Scientific and technical findings by NASA-sponsored contractors and grantees.

- CONFERENCE PUBLICATION. Collected papers from scientific and technical conferences, symposia, seminars, or other meetings sponsored or co-sponsored by NASA.

- SPECIAL PUBLICATION. Scientific, technical, or historical information from NASA programs, projects, and missions, often concerned with subjects having substantial public interest.

- TECHNICAL TRANSLATION. English-language translations of foreign scientific and technical material pertinent to NASA's mission.

Specialized services also include organizing and publishing research results, distributing specialized research announcements and feeds, providing information desk and personal search support, and enabling data exchange services.

For more information about the NASA STI program, see the following:

- Access the NASA STI program home page at http://www.sti.nasa.gov

- E-mail your question to help@sti.nasa.gov

- Phone the NASA STI Information Desk at 757-864-9658

- Write to:
  NASA STI Information Desk
  Mail Stop 148
  NASA Langley Research Center
  Hampton, VA 23681-2199

NASA/TM–2020-5003145

# Progressive Failure Analysis Correlation with Notched Composite Laminate Test Data

*Arunkumar Satyanarayana and Sandra P. Walker*
*Langley Research Center, Hampton, Virginia*

*Kevin E. Gould*
*Analytical Mechanics Associates, Inc., Hampton, Virginia*

National Aeronautics and
Space Administration

Langley Research Center
Hampton, Virginia 23681-2199

June 2020

Available from:

NASA STI Program / Mail Stop 148
NASA Langley Research Center
Hampton, VA 23681-2199
Fax: 757-864-6500

# Progressive Failure Analysis Correlation with Notched Composite Laminate Test Data

## Nomenclature

| | |
|---|---|
| $E_1$ | *Modulus in 1 direction* |
| $E_2$ | *Modulus in 2 direction* |
| $G_{12}$ | *Shear Modulus* |
| $v_{12}$ | *Poisson's Ratio* |
| $\sigma_{11}$ | *Stress in 1 direction (Axial)* |
| $\sigma_{22}$ | *Stress in 2 direction (Transverse)* |
| $\sigma_{12}$ | *Stress in 1-2 plane (Shear)* |
| $\varepsilon_{11}$ | *Strain in 1 direction (Axial)* |
| $\varepsilon_{22}$ | *Strain in 2 direction (Transverse)* |
| $\varepsilon_{12}$ | *Strain in 12 direction (Shear)* |
| $X_T$ | *Fiber strength in Tension* |
| $X_C$ | *Fiber strength in Compression* |
| $Y_T$ | *Matrix strength in Tension* |
| $Y_C$ | *Matrix strength in Compression* |
| $S_{12}$ | *Matrix shear strength* |
| $X$ | *Fiber Strength* |
| $Y$ | *Matrix Strength* |
| $Gc$ | *Fracture Toughness* |
| $df$ | *Fiber damage index* |
| $dm$ | *Matrix damage index* |
| $Vm$ | *Matrix volume fraction* |

***Abstract***

*Testing of small and intermediate laminate panels with notches was performed and Progressive Failure Analyses (PFA) models were developed for aid in test planning and for correlation with the test data. Two progressive damage failure models were included in the study: the commercially available Abaqus built-in damage model and COmplete STress Reduction (COSTR) damage model developed at NASA Langley Research Center (LaRC). The finite elements models used for the analysis were developed using shell elements. The pre-test PFA results obtained from the two damage models were compared to test data. Then a post-test PFA with updated material properties based on additional available material property data was executed with the COSTR damage model and compared to the test data. The panels tested in compression all exhibited less scatter in the failure load with self-similar failure behavior. The panels tested in tension exhibited more scatter in the failure load with a failure mode that included delamination of plies. However, a self-similar crack path was also observed as the overall failure mode for all panels tested. When comparing test data to the pre-test analysis results, both damage models with shell element models were considered adequate for predicting the behavior and failure load of both the small and intermediate panels when tested in compression. However, for the tension load cases, larger differences were observed between the test and analysis results. When comparing test data to the post-test analysis performed using the COSTR damage model, better correlation was observed. However, large discrepancies were still observed for the tension load cases. Consequently, a higher fidelity finite element model including solid elements for sub-laminates and the modeling of cohesive layers between sub-laminate layers is recommended for tension loading of notched composite laminates.*

# I. Introduction

The development of damage tolerant aircraft structure requires the structure to continue to carry design loads when damage occurs in the form of large notches penetrating the structure. However, prediction of the residual strength of a stiffened composite panel with a notch is complex and challenging. Progressive Failure Analysis (PFA) methods are needed to predict the complex damage progression occurring in the composite material that leads to ultimate failure of the structure's ability to carry any load [1]. However, PFA techniques have been historically unreliable in predicting failure progression [2]. Creating and executing high fidelity PFA finite element models is also laborious, time consuming, and costly. Additionally, testing of stiffened panels with large notches is challenging, expensive, and time consuming regarding the design and fabrication of the panel and test fixtures. Therefore, to consider residual strength early in the design phase and to consider a sufficiently large design space, a more rapid, closed form approach to predicting the residual strength of stiffened panels with large notches is desirable.

Closed-form approaches have been developed that require just the unstiffened notched panel strength to predict the stiffened panel residual strength [1]. Furthermore, the unstiffened notched panel strength can then be assessed with the use of the Mar-Lin curve [3]. Mar-Lin developed a semi-empirical method, to predict residual strength of a notched unstiffened panel provided there exist residual strength values for two of the same, but smaller sized panels with consecutively smaller notch lengths. This approach is suitable for design engineers since testing small notched panels to obtain their residual strength is relatively simpler, faster, and less expensive than testing unstiffened, or more so stiffened panels, with large notches.

To evaluate the PFA approach for consideration in predicting the residual strength of a large, 40-inch wide stiffened panel with a 2-bay, 8-in. notch length, tests of unstiffened notched laminates, both in tension and compression were performed for two panels, referred to as small and intermediate [4]. The small panels were 4-in. wide with a 0.8-in. notch length, and the intermediate panel was 20-in. wide with a 4.-in. notch length. Then, these strengths can be used in generating a Mar-Lin curve to predict failure strength of a 40-in., wide unstiffened panel with an 8 in. notch length, which can subsequently be used as input to obtain residual strength of a stiffened panel using a closed-form approach.

The focus of this study was to perform PFA of the small and intermediate notched laminates to predict both the failure load and mode of the laminate test panels. The objective of the PFA effort was to both aid in the planning of the tests and to evaluate the effectiveness of two PFA methods with relatively simply finite element models (FEMs) to predict notched laminate failure load and mode. The two PFA methods included in this evaluation included: the commercially available Abaqus built-in damage model [5] and the COmplete STress Reduction (COSTR) [6] damage model developed at NASA Langley Research Center (LaRC). Both damage models were used herein to perform pre-test predictions of the small and intermediate notched laminates under tensile and compressive loads. Finite element models (FEMs) using two-dimensional shell elements were constructed for use with PFA and the analysis results were compared to the existing test data to evaluate the effectiveness of PFA to predict failure progression in the laminates. The two-dimensional finite element models (FEMs) developed here for use with the PFA damage models are relatively simple to construct and less costly to execute than higher fidelity FEMs that utilize three-dimensional elements with additional cohesion elements to more accurately capture progressive damage.

Furthermore, post-test analysis using COSTR damage model and updated material properties from additional available material property data sources was performed. The purpose of this effort was to identify the best set of material properties to accurately capture the failure load of the panels. This property set could then be used in modeling stiffened composite panels with a center notch that were being fabricated for testing. Models of the stiffened panels were also needed for planning those tests.

Details of the unstiffened test panel configurations and data measurement system are described in the next section. Reduced test data is then presented, discussed, and evaluated. The following section introduces the progressive failure analysis effort which includes a sub-section summarizing the damage models utilized for this study and a sub-section presenting information on the finite element models developed for the analysis. The results of both a pre-test and then a post-test updated analyses are then presented and compared to the test results, which includes some discussion.

# II. Test Panel Configuration and Data Measurement Systems

The small and intermediate test panels were made using IM7/8552 material system prepreg tape. The laminates were all constructed with a [45/90/-45/0$_2$/45/90/-45/0]s layup and 18 plies, resulting in an average laminate thickness of 0.129 in. In-plane global dimensions of the actual test panels are presented in Table 1 along with the load type. More complete dimensions of the test panels along with strain gauge location are presented in Figure 1. The green color regions in the figure represent tab ends.

The test panels had back-to-back strain gauges at the notch tips and far-field locations. Eight inch long extension transducers on either longitudinal edges were installed on the tension panels to measure axial displacement. The compression panels were sandwiched between two 0.25-in., thick steel plates with cut-outs around the notch region and far-field strain gauge location. These plates were used to prevent out-of-plane deformation and premature buckling of the panels. A photograph of the compression test fixture utilized for testing the small panels is presented in Figure 2.

**Table 1: Test Panel Specifications.**

| Panel Specification | Notch Length (in.) | Width (in.) | Length (in.) | No of Replicates | Load Type |
|---|---|---|---|---|---|
| Small | 0.8 | 4 | 12 | 3 | Compression |
| Small | 0.8 | 4 | 12 | 3 | Tension |
| Intermediate | 4.0 | 20 | 60 | 2 | Compression |
| Intermediate | 4.0 | 20 | 60 | 2 | Tension |

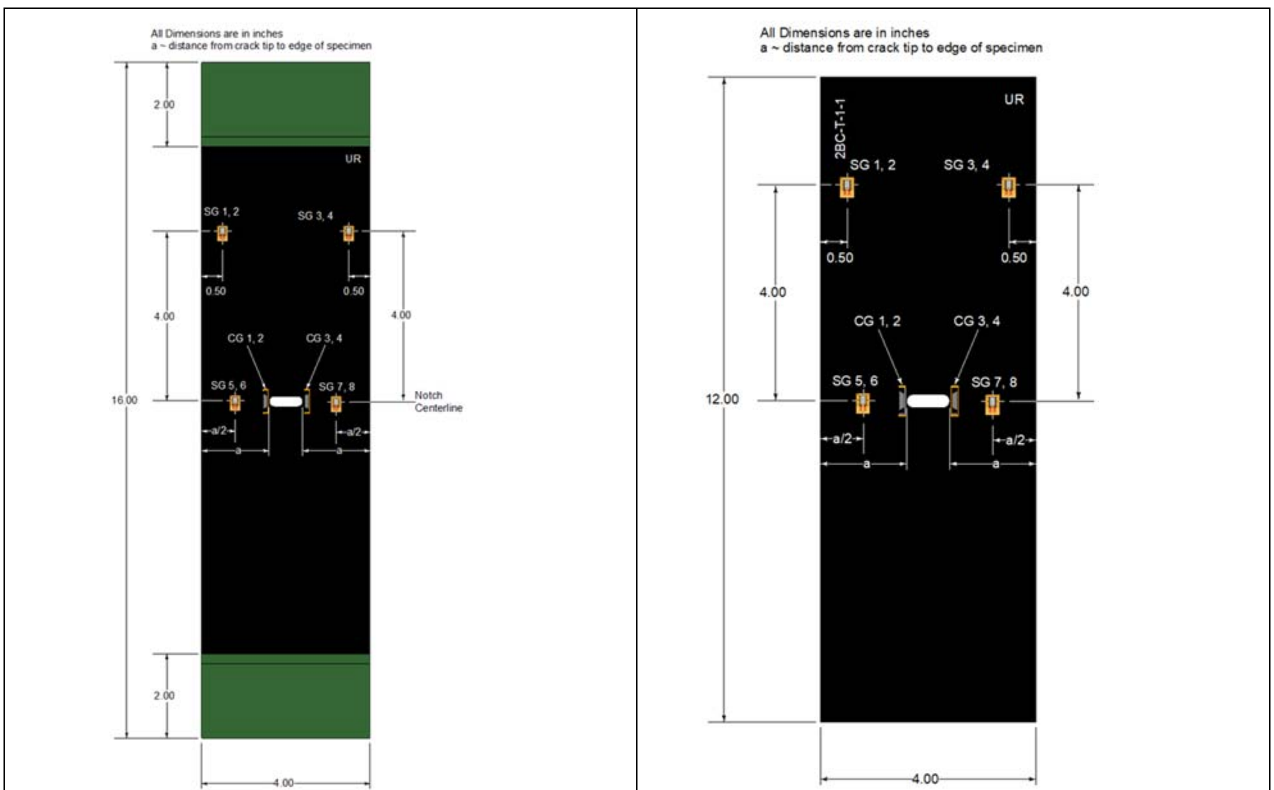


**a. Tension Panel**

**b. Compression Panel**

**Figure 1:Dimensions and Strain Gauge Layout of the Small Test Panels.**

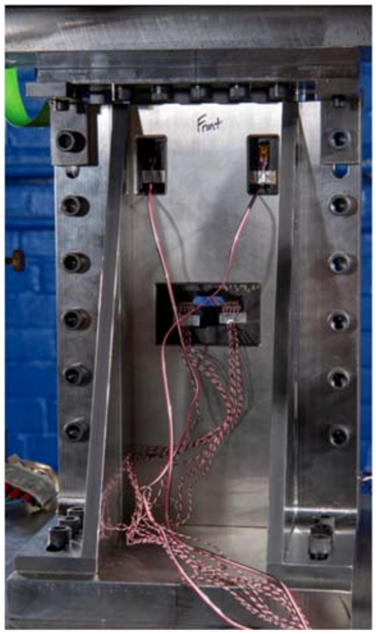


**Figure 2:Test Setup for Small Compression Panels.**

Dimensions and the location of strain gauges for the intermediate tension panels along with end tabs is presented in Figure 3a. Test fixture hardware included back-to-back longitudinal square cross-section rods which were placed in contact with the panel near the notch with help of C-channels is shown in Figure 3b. This setup was used for tension panels to minimize bulging of the notch region.

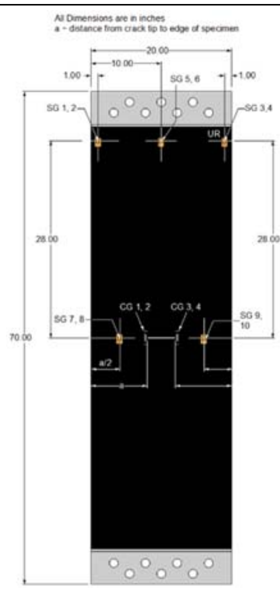


**a. Intermediate Tension Panel**

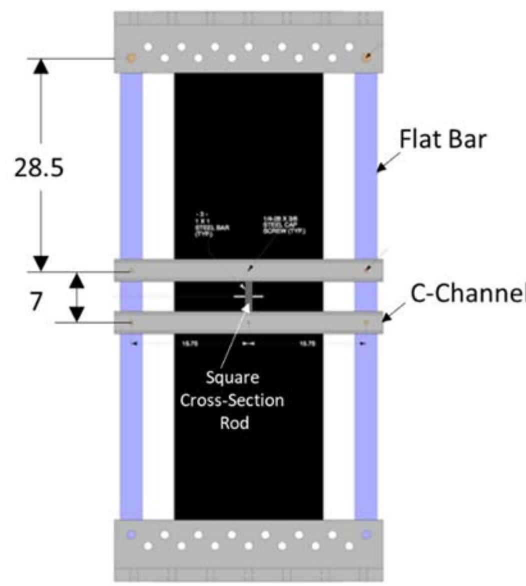


**b. Test Setup**

**Figure 3:Dimensions and Strain Gauge Layout of Intermediate Tension Panel and Tension Test Setup.**

The test setup of intermediate compression panel is not shown here due to proprietary nature of the design. A small strip of region near the notch was left free where the rest of the panel was constrained in the out-of-plane direction in order to prevent pre-mature buckling.

## III. Test Results of Notched Panels

Tension and compression tests of the small panels and the tension test of the intermediate panels were performed at NASA LaRC and the compression tests of the intermediate panels was performed at a Boeing facility. All panels were tested under displacement control mode. The failure loads of the small test panels are given in Table 2 and the failure loads of the intermediate test panels are given in Table 3.

**Table 2: Failure Load of Small Test Panels.**

| Panel ID | Load Type | Notch Length (in.) | Test Failure Load (kips) | Average Test Failure Load (kips) |
|---|---|---|---|---|
| 2BC-C-1-1 | Compression | 0.8 | 18.40 | 18.16 |
| 2BC-C-1-2 | Compression | 0.8 | 18.39 | |
| 2BC-C-1-3 | Compression | 0.8 | 17.68 | |
| 2BC-T-1-1 | Tension | 0.8 | 34.10 | 33.80 |
| 2BC-T-1-2 | Tension | 0.8 | 33.05 | |
| 2BC-T-1-3 | Tension | 0.8 | 34.24 | |

**Table 3: Failure Load of Intermediate Test Panels.**

| Panel ID | Load Type | Notch Length (in.) | Failure Load (kips) | Average Failure Load (kips) |
|---|---|---|---|---|
| 2BC-C-4-1 | Compression | 4.0 | 53* | 52.55 |
| 2BC-C-4-2 | Compression | 4.0 | 52.1 | |
| 2BC-T-4-1 | Tension | 4.0 | 102.16 | 109.95 |
| 2BC-T-4-2 | Tension | 4.0 | 117.74 | |

* Adjusted test data based on engineering analysis.

For the small panels tested, based on the data shown in Table 2, the average compression test failure load is 18.16 kips with test values ranging from -2.6% to +1.3% of average. Similarly, the average tension test failure load is 33.8 kips with test values ranging from -2.2% to +1.3% of the average value.

For the intermediate panels tested under compression at Boeing, significant bending was noticed in one of the panels (2BC-C-4-1) from the beginning of the loading cycle and ultimately failed at 44.2 kips. However panel 2BC-C-4-2 showed normal bending behavior, and based on failure strain of this panel, the failure strain of 2BC-C-4-1 was modified based on engineering analysis [7], which led to adjusting the failure load to 53 kips. Thus the average adjusted test failure load of the intermediate panel under compressive load is 52.55 kips.

For the intermediate panels tested under tension load at LaRC, the average test failure load is 109.95 kips. In addition to the large difference of 13.2% between the two failure loads, both the panels exhibited noticeable nonlinear behavior with an increase in stiffness. Far-field strain gauge data of both the panels are presented in Figure 4, where the nonlinear increase in stiffness can be observed occurring for Panel-1 in Figure 4a, and Panel-2 in Figure 4b. In general, for a uniform loading scenario, strain data from gauges 1-6 (far-field) ideally should exhibit linear behavior until failure, and should have similar strain values. However, the middle gauges (SG-5, 6) located right above the notch may record a lesser value. The stiffening behavior was noticed in panel-1 (see Figure 4a) with slight increase in stiffness at approximately 60 kips. Also, slippage of the test panel was noticed during the test at approximately 92 kips and is reflected in the load versus end displacement curve in the form of load oscillations. Regarding panel-2 (Figure 4b), a strain jump (strain relaxation) was noticed at approximately 60 kips in gauges 1-4, which was approximately half the final failure load. This behavior could be attributed to a potential slippage between panel and the loading fixture. In addition to this jump, the middle gauges (SG-5, 6) are reading higher strains than gauges 1-4.

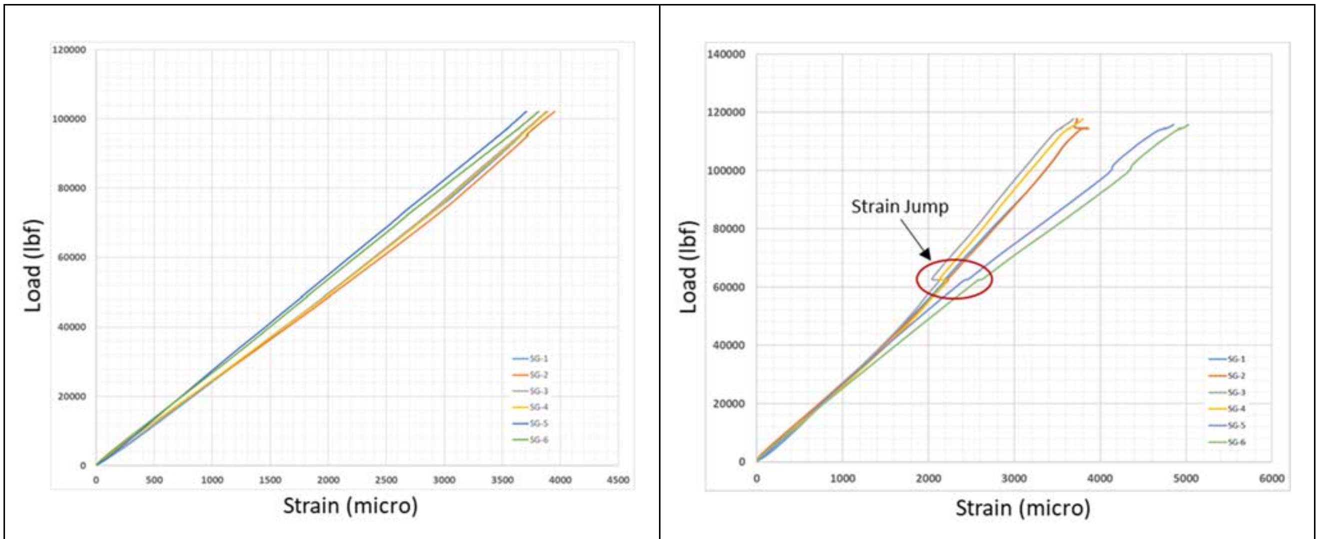


| a. 2BC-T-4-1 Panel | b. 2BC-T-4-2 Panel |
|---|---|

**Figure 4: Far-Field Strain Data of Intermediate Tension Panels.**

In general, failure mode of all panels was a through thickness self-similar crack, i.e., the crack path of the laminate load carrying plies is perpendicular to the loading direction; and the crack starts from the notch tips and then propagates all the way to the edge. Additionally, crack path in laminates is categorized as self-similar when fibers are fractured in all the plies, or at least in load carrying plies, which in this case are the $0^{o}$ plies; combined with matrix failure in non-$0^{o}$ plies and delamination confined along the crack path between some or all ply interfaces. Photographs of failed panels with typical results are presented in Figure 6. Note that the outer surface ply that is visible in the photographs is a $45^{o}$ ply which delaminated from the underlying plies, and which masks the self-similar nature of the underlying failure mode of the panel.

| | |
|---|---|
| 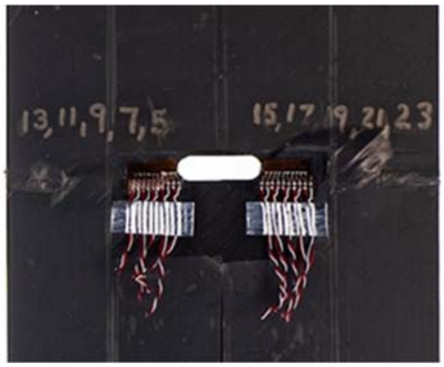 |  |
| Small Panel under Compression | Small Panel under Tension |
| 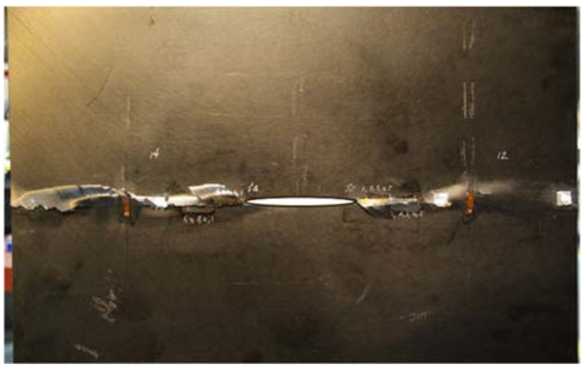 | 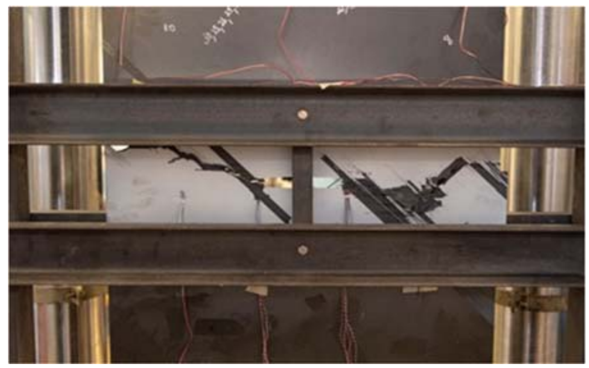 |
| Intermediate Panel under Compression | Intermediate Panel under Tension |

**Figure 6: Crack Path in Failed Small and Intermediate Test Panels.**

## IV. Progressive Failure Analysis Methodology

### a. Damage Models

Progressive failure analysis (PFA) of notched panels was performed with Abaqus Built-in [5] and COmplete STress Reduction (COSTR) [6] damage models to obtain failure load predictions for use in test planning, and to assess overall stiffness and structural response. The Abaqus Built-in damage model, which is commercially available is briefly described here. For a detailed explanation of the model, one can refer to Abaqus theory manual [5]. In general, the Abaqus damage model adopts Hashin [8] and Hashin-Rotem [9] failure criterion to identify damage initiation. The stress degradation approach used to simulation damage is shown in figure 7.

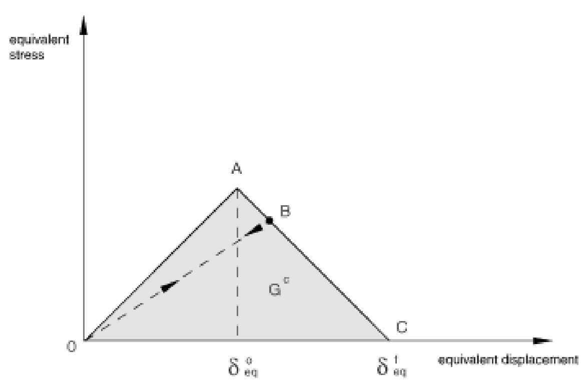


**Figure 7: Stress Degradation Profile of Abaqus Built-in Damage Model.**

The damage variable evolves based on the stress displacement behavior as shown in Figure 7 for all damage modes (fiber and matrix). Point A in Figure 7 represents the material strength and damage initiation point. The area of the triangle is related to energy required to fail the material completely, which is equivalent to the fracture toughness parameter (Gc) provided by the user. The stress degradation profile after damage initiation, point A, follows the linear curve AC. Line OB shows the loss in stiffness due to damage initiation and the unloading path due to load removal that might occur before complete damage.

As an alternative to the Abaqus Built-in damage model, the COSTR damage model was developed at NASA Langley Research Center to simulate intra-laminar damage such as fiber and matrix failure [6]. The COSTR damage model is interfaced with the Abaqus/Explict solver utilizing an Abaqus user-written subroutine, VUMAT.

The progressive failure analysis procedure adopted in the COSTR damage model consists of three steps. The first step is to determine damage in an element at each and every ply. This was accomplished by adopting the Hashin-Rotem failure criteria [9]:

***Fiber Damage:*** *Tension & compression*

$$\left(\frac{\sigma_{11}}{X_T}\right) \geq 1 \; for \; \sigma_{11} \geq 0 \, , df = 1.0 \qquad \left(\frac{\sigma_{11}}{X_C}\right) \geq 1 \; for \; \sigma_{11} < 0 \, , df = 1.0$$

***Matrix Damage:*** *Tension , compression & Shear*

$$\left(\frac{\sigma_{22}}{Y_T}\right)^2 + \left(\frac{\sigma_{12}}{S_{12}}\right)^2 \geq 1 \; for \; \sigma_{22} \geq 0 \, , dm = 1.0 \qquad \left(\frac{\sigma_{22}}{Y_C}\right)^2 + \left(\frac{\sigma_{12}}{S_{12}}\right)^2 \geq 1 \; for \; \sigma_{22} \leq 0 \, , dm = 1.0$$

The damage indices *df* and *dm* represent the damage status of fiber and matrix material systems, respectively. Damage index *df* will be zero while the fiber damage criteria is less than 1, and then attains a value of 1 when the fiber damage criteria becomes greater or equal to 1. A similar procedure is adopted for the matrix damage index *dm*. The constitutive law along with damage indices is presented below.

$$\begin{pmatrix} \sigma(11) \\ \sigma(22) \\ \sigma(12) \end{pmatrix} = \begin{pmatrix} (1-0.8(df))Q11 & (1-df)(1-dm)Q12 & 0. \\ (1-df)(1-dm)Q12 & (1-df)(1-dm)Q22 & 0. \\ 0. & 0. & (1-df)(1-Vmdm)Q66 \end{pmatrix} \begin{pmatrix} \varepsilon\,(11) \\ \varepsilon\,(22) \\ \varepsilon\,(12) \end{pmatrix}$$

$Q11 = E_1 / \Delta$
$Q22 = E_2 / \Delta$
$Q12 = \nu_{12} E_2 / \Delta$
$Q66 = G_{12}$
$\Delta = [1 - \nu_{12}\nu_{21} (1 - dm)]$

Once stress in an element for a ply reaches the ply strength, the stress is degraded as show in Figure 8. Damage simulation of the fiber is accomplished by instantaneously reducing the axial stress, ($\sigma_{11}$), to 20% of the axial strength, X, and then maintaining that level until the area under the stress strain curve when multiplied by the characteristic length of an element, equates to the fiber fracture toughness ($G_{Fc}$). However, when the transverse stress, ($\sigma_{22}$), reaches the transverse strength, Y, the transverse stress, ($\sigma_{22}$), is instantaneously reduced to zero, but the shear stress, ($\sigma_{12}$), is reduced by an amount proportional to the resin volume fraction in plies where the fibers are not aligned with the loading direction, and to zero level in plies where the fibers are aligned parallel to the loading direction. In the case of matrix damage, when the shear stress, ($\sigma_{12}$), reaches the shear strength, S, then both transverse stress, ($\sigma_{22}$), and shear stress, ($\sigma_{12}$), are instantaneously reduced to zero. Additional information regarding shear stress degradation due to matrix damage can be found in reference [10]. The failure load provided by this damage model is independent of finite element area [6].

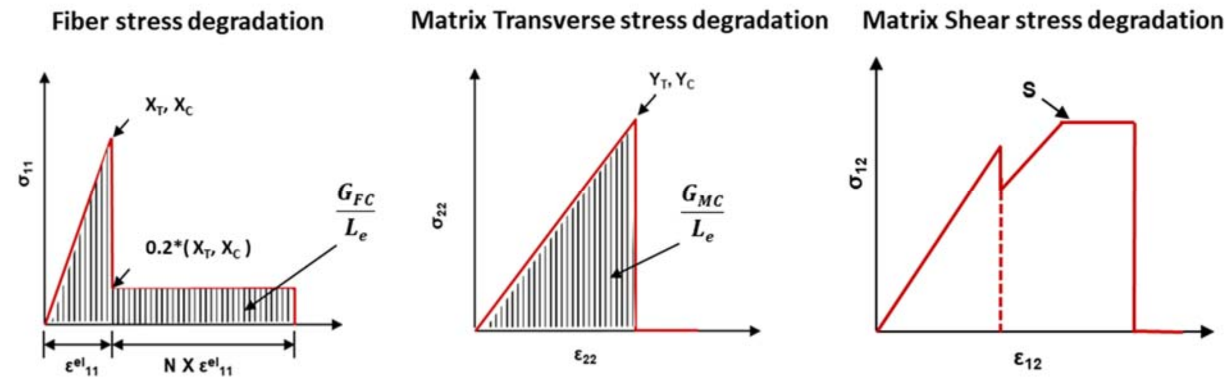


**Figure 8: Stress Degradation Profiles in COSTR Damage Model.**

The final step in PFA is simulation of the virtual crack. This step is accomplished by deleting elements from computation when fibers in all the plies have been damaged. In certain plies, where fibers are not damaged but matrix is, a quadratic strain criterion involving transverse and shear strains is adopted and is set to a large value greater than 0.2 in./in., in flagging failure of the ply.

In general, both damage models have the same in-plane failure criteria. However, the stress degradation profile is significantly different between the two damage methods. The Abaqus built-in damage model has a gradual stress degradation profile after damage (fiber and matrix) initiation. Also, Abaqus built-in uses one fiber fracture toughness value, which does not accommodate the use of both fiber fracture initiation and propagation values, when available. However, the COSTR damage model is capable of using both fiber fracture, initiation and propagation values and has different stress degradation profiles for fiber and matrix damage simulation.

### b. Progressive Failure Analysis Model of Small and Intermediate Panels

Finite element models (FEM) of the small and intermediate panels were generated for performing both compression and tension analysis using the Abaqus explicit finite element code. The general panel specifications for the small and intermediate panels are listed in Table 1. The COSTR finite element models are presented in Figure 9 for small and intermediate panels for both the tension and compression analysis. The panel's left edge is fixed in all degrees of freedom (DOF) and the right edge is fixed for all DOF except for the axial DOF. An axial displacement is applied to the right edge of the panels. For the compression panels, all the interior nodes except a small window near the notch area are fixed in the out-of-plane direction (highlighted in orange color). In the case of the intermediate tension panel, a few nodes near the notch are fixed in the out-of-plane direction to represent the out-of-plane constraint imposed by the rod shown in Figure 3b, which was designed to prevent buckling near the notch during testing. The notch width is 0.25 in. in all models and the notch tips all have a radius of 0.125 in. at the ends. The material properties and strengths used in the pre-test PFA are given in Table 4 [2]. Average modulus values in 1, 2 direction and average value of Poisson's ratio were used in the analysis by both damage models. Identical properties and strengths are used by both the damage models except fiber and matrix fracture toughness values. Fiber and matrix fracture toughness properties in tension and compression used in the Abaqus built-in damage model is half of what is used for the COSTR damage model and this approach was based on past experience and best modeling practices when using Abaqus. The fracture initiation values used in the COSTR damage model are evaluated based on Bazant's equation provided in the Abaqus manual [5] for a characteristic distance of 0.09-in. The FEM of the panels were generated using S4R Abaqus shell elements. The maximum element length is approximately 0.125 in. The FEM used with the Abaqus built-in damage model has the same global dimensions, boundary and load conditions as shown in Figure 9, but different element sizes are used. The Abaqus Built-in FEM consists of elements whose maximum length is approximately 0.08in. Evaluation of maximum element size is based on Bazant's equation provided in the Abaqus manual [5] and depends on fracture toughness properties. Since the damage evolution and mesh regularization procedures are different between the Abaqus built-in and COSTR damage models, the latter can accommodate larger element sizes.

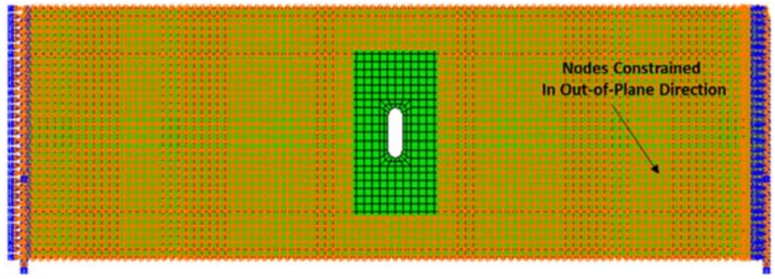


Small Compression Panel

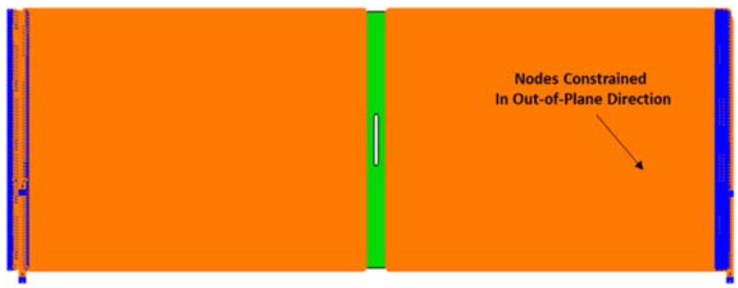


Intermediate Compression Panel

a: Small and Intermediate Compression Panels.

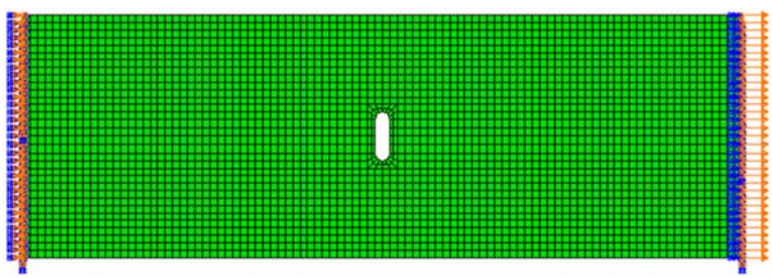

Small Tension Panel

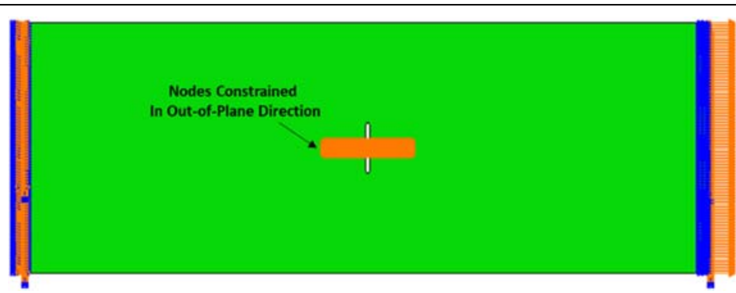


Intermediate Tension Panel

b: Small and Intermediate Tension Panels.

**Figure 9: COSTR Finite Element Models of Small and Intermediate Panels.**

**Table 4: Properties and Strengths of IM7/8552-1 lamina used in Pre-Test PFA.**

| Properties | Abaqus Built-in | COSTR |
|---|---|---|
| E1t (Msi) | 22.14 | 22.14 |
| E1c (Msi) | 20.04 | 20.04 |
| E1Avg (Msi) | 21.27 | 21.27 |
| E2t (Msi) | 1.26 | 1.26 |
| E2c (Msi) | 1.41 | 1.41 |
| E2Avg (Msi) | 1.335 | 1.335 |
| Nu12t | 0.32 | 0.32 |
| Nu12c | 0.356 | 0.356 |
| Nu21 | 0.024 | 0.024 |
| Nu23 | 0.45 | 0.45 |
| G12 (Msi) | 0.749 | 0.749 |
| G13 (Msi) | 0.749 | 0.749 |
| G23 (Msi) | 0.435 | 0.435 |
| Xt (Ksi) | 337.0 | 337.0 |
| Xc (Ksi) | 248.94 | 248.94 |
| Yt (Ksi) | 11.6 | 11.6 |
| Yc (Ksi) | 41.8 | 41.8 |
| Sxy (ksi) | 14.2 | 14.2 |
| $Gc^{fT}$ (in-lbf/in$^2$) | 385.45 | 240 / 771 |
| $Gc^{fC}$ (in-lbf/in$^2$) | 228.5 | 131 / 457 |
| $Gc^{mT}$ (in-lbf/in$^2$) | 2.25 | 4.5 |
| $Gc^{mC}$ (in-lbf/in$^2$) | 29.5 | 59.0 |

## V. Results and Discussion

### a. Comparison of Test Results to Pre-Test PFA

The pre-test analysis results are presented in Table 5 along with test data. Based on comparison of analysis and test results, the PFA results mostly over-predicted the failure load for compression load cases and under-predicted the failure load for tension load cases. This trend was consistent for small panels with both damage models, while there was a slight under-prediction by COSTR for the intermediate panel tested in compression. Considering the compression results, correlation between test and PFA analysis is considered to be adequate with the maximum difference of 11.3% occurring for the small panels when compared to COSTR PFA results. Considering the tension results, the maximum difference was near 40%, and both damage models significantly under-predicted the test failure load. Consequently, the pre-test PFA analysis models are not considered adequate to accurately predict the failure load of the notched composite laminates when tested in tension. Additionally, all analysis performed predicted a self-similar type failure mode originating at the notch tip, which agreed with the test results.

**Table 5: Comparison of Pre-Test Failure Load Predictions of Panels with Test Data.**

| Notch Size | Load Case | Average Test Failure Load (kips) | Pre-Test Failure Load COSTR (kips) | Pre-Test Failure Load Abaqus Built-in (kips) | % Error COSTR | % Error Abaqus Built-in |
|---|---|---|---|---|---|---|
| Small | Compression | 18.16 | 20.22 | 19.9 | +11.30 | +9.60 |
| Small | Tension | 33.80 | 28.89 | 24.65 | -14.53 | -27.10 |
| Intermediate | Compression | 52.55* | 52.31 | 53.20 | -0.46 | +1.24 |
| Intermediate | Tension | 109.95 | 70.51 | 65.80 | -35.87 | -40.15 |

*Average of adjusted test data based on engineering analysis.

**b. Post-Test PFA and Material Property Adjustments**

Due to the large differences observed in some cases between the pre-test PFA predicted and test results, further investigation into the possible causes ensued by interrogating the material properties chosen for the pre-test analysis. The purpose of this effort was to identify a material property input set that better represented the actual panel material properties, and that should subsequently be used in future analyses to better predict panel behavior. Considering the fiber direction strength data in tension (Xt = 337 ksi) as reported in Table 4, the value was observed to be low when compared with other material data sources from Hexcel [11] and NIAR [12], where the data sheets are presented in the appendix. Hexcel and NIAR reported tensile strength of unidirectional lamina as 395 ksi and 371.08 ksi, respectively, at room temperature. However, NIAR [12] reported an Xt of 320.79 ksi for an un-notched tension laminate (UNT0) which is close to the value (337.0 ksi) used in pre-test analysis. The UNT0 coupons are 0/90 laminate and the strengths are back calculated from Classical Laminate Theory (CLT) expressions. So, the Xt = 371 ksi value obtained from NIAR of the unidirectional lamina was used in the post-test PFA rather than a value of 337.0 ksi which was used in the pre-test analysis. Next, the fiber-direction compression strength, Xc = 248.94 ksi, used in the pre-test analysis was also obtained from 0/90 cross-ply laminate coupons. However, unlike for Xt, there was no data available for Xc from unidirectional laminates in the material property reference documents used here. Hence, considering the pre-test PFA over-predicting the test panel failure load as presented in Table 4, Xc was reduced to 215.0 ksi for the post-test PFA prediction. This value was chosen based on several PFA predictions performed using COSTR damage model to determine a value that resulted in a failure load that better matched the small compression test data. Then post-test PFA analysis was performed just with COSTR damage model. The fiber fracture toughness values reported in reference [2] are used in the post-test analysis for $Gc^{fT}$ and $Gc^{fC}$. However the fracture toughness values of $Gc^{mT}$ and $Gc^{mC}$ were evaluated using Bazant's [13] energy equation for a characteristic distance of 0.09-in. The modified strengths and properties used in post -test PFA are given in Table 6. Measured values are used when normalized values are not available for some properties and strengths. The highlighted cell indicates values that are changed from the pre-test data set where for this set the properties and strengths are now taken from Reference [12] unless already discussed otherwise. However the same finite element models used in the pre-test analysis were used during the post-test analysis when employing Abaqus built-in and COSTR damage models.

**Table 6: Properties and Strengths of IM7/8552-1 used in Pre- and Post-Test PFA**

| Properties | Pre-Test Abaqus | Post-Test Abaqus | Pre-Test COSTR | Post-Test COSTR |
|---|---|---|---|---|
| E1t (Msi) | 22.14 | 22.99 | 22.14 | 22.99 |
| E1c (Msi) | 20.04 | 20.04 | 20.04 | 20.04 |
| E1Avg (Msi) | 21.27 | 21.52 | 21.27 | 21.52 |
| E2t (Msi) | 1.26 | 1.3 | 1.26 | 1.3 |
| E2c (Msi) | 1.41 | 1.41 | 1.41 | 1.41 |
| E2Avg (Msi) | 1.335 | 1.355 | 1.335 | 1.355 |
| Nu12t | 0.32 | 0.316 | 0.32 | 0.316 |
| Nu12c | 0.356 | 0.356 | 0.356 | 0.356 |
| G12 (Msi) | 0.749 | 0.68 | 0.749 | 0.68 |
| G13 (Msi) | 0.749 | 0.68 | 0.749 | 0.68 |
| G23 (Msi) | 0.435 | 0.435 | 0.435 | 0.435 |
| Xt (Ksi) | 337.0 | 371.08 | 337.0 | 371.08 |
| Xc (Ksi) | 248.94 | 215.0 | 248.94 | 215.0 |
| Yt (Ksi) | 11.6 | 9.29 | 11.6 | 9.29 |
| Yc (Ksi) | 41.8 | 41.44 | 41.8 | 41.44 |
| Sxy (ksi) | 14.2 | 13.22 | 14.2 | 13.22 |
| $Gc^{fT}$ (in-lbf/in$^2$) | 385.45 | 585 | 240 / 771 | 282 / 1170 |
| $Gc^{fC}$ (in-lbf/in$^2$) | 228.5 | 174 | 131 / 457 | 130 / 348 |
| $Gc^{mT}$ (in-lbf/in$^2$) | 2.25 | 1.435 | 4.5 | 2.87 |
| $Gc^{mC}$ (in-lbf/in$^2$) | 29.5 | 28.5 | 59.0 | 57.0 |

The failure loads from the post-test PFA using the COSTR and Abaqus built-in damage models are presented in Table 7 and 8 for small and intermediate panels, respectively. Considering the small panels, the failure load prediction by COSTR damage model was within 1% and 12% for compression and tension cases, respectively. Since the COSTR model of the small panel was tuned to predict compression failure load for the small panel by adjusting Xc for the post-test analyses, the close prediction for the small panel tested in compression was expected. For the intermediate panels, the failure load was under-predicted for the compression load case by approximately 8% when compared to average test data and the failure load was under-predicted for the tension load case by approximately 23% when compared to average test data.

Similar trend was noticed in the failure load predictions by Abaqus built-in damage model. In case of small panels, the failure load over prediction was within 2% and under prediction of 16% for compression and tension cases, respectively. For the intermediate panels, the failure load was under-predicted for the compression load case by approximately 12% when compared to average test data and the failure load was under-predicted for the tension load case by approximately 26.3% when compared to average test data.

In general, failure load predictions are improved using the post-test material property data set. Consequently, this data set is recommended for future analyses of panels constructed from the same laminate material with COSTR damage model. Considering just the post-test results, failure load prediction is better with respect to compression load cases than tension load cases. For the tension load tests, under-prediction of the failure load is considered to be due to the limitation of the finite element models. During testing of the small and intermediate panels in tension, the delamination occurring at certain ply interfaces, as was shown in Figure 6, would have caused the stress reduction at the notch tips and have extend the failure load. To improve the prediction of failure load of tension panels, higher fidelity models, using solid elements with cohesive elements at certain ply interfaces, are recommended for future studies to better predict failure.

**Table 7: Failure Load of Small Panels from Post-Test Progressive Failure Analysis.**

| Notch Size | Load Case | Average Actual Test Failure Load (kips) | Post-Test Failure Load COSTR (kips) | Post-Test Failure Load Abaqus Built-in (kips) | % Error COSTR | % Error Abaqus Built-in |
|---|---|---|---|---|---|---|
| Small | Compression | 18.16 | 17.99 | 18.51 | -0.936 | +1.93 |
| Small | Tension | 33.80 | 29.85 | 28.50 | -11.68 | -15.68 |

**Table 8: Failure Load of Intermediate Panels from Post-Test Progressive Failure Analysis.**

| Notch Size | Load Case | Average Test Failure Load (kips) | Post-Test Failure Load COSTR (kips) | Post-Test Failure Load Abaqus Built-in (kips) | % Error COSTR | % Error Abaqus Built-in |
|---|---|---|---|---|---|---|
| Intermediate | Compression | 52.55* | 48.43 | 46.24 | -7.84 | -12.00 |
| Intermediate | Tension | 109.95 | 84.66 | 81.04 | -23.0 | -26.29 |

*Average of adjusted test data based on engineering analysis.

The crack path predicted by the COSTR model with post-test properties is presented in Figure 10. The model predicts self-similar crack for all cases evaluated which agreed with the test results. However, simulation of delamination is not possible with shell models as this failure mode is not available. Consequently, as noted earlier, this could be the reason for the discrepancies between PFA predicted and test failure load of both small and intermediate tension panels. The evidence of delamination is prominent in small tension panel which is shown in Figure 4, where the damage region is widely spread.

The crack path predicted by the Abaqus built-in damage model with post-test properties is identical to the one presented in Figure 10 and hence, is not presented in this report. However, the model predicts self-similar crack in all coupons and for all load cases evaluated which agreed with the test results.

| | |
|---|---|
| 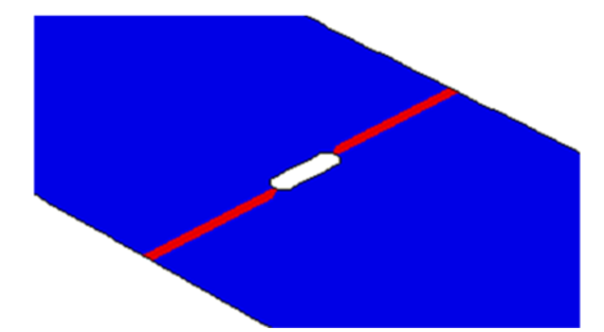 | 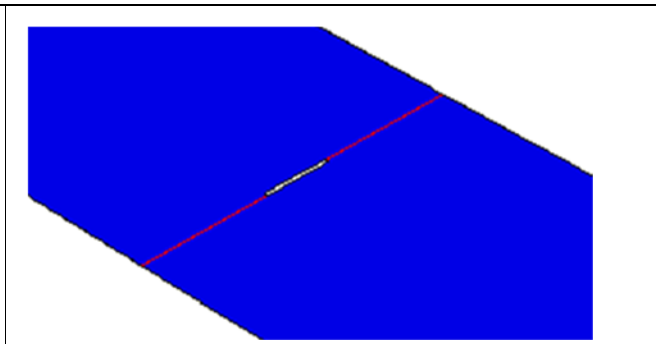 |
| Small Compression Panel – COSTR Damage Model | Intermediate Compression Panel – COSTR Damage Model |
| 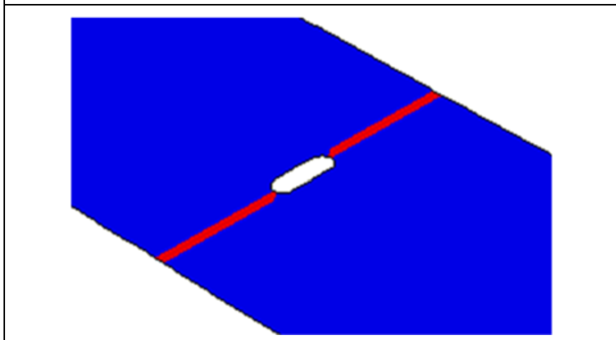 | 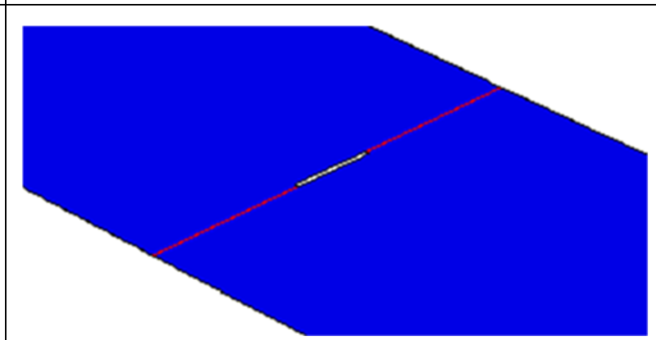 |
| Small Tension Panel – COSTR Damage Model | Intermediate Tension Panel – COSTR Damage Model |

**Figure 10: Crack Path (Fiber Damage) Predictions by COSTR Damage model**

In Figure 11, the load versus end displacement response obtained from a typical test of a small panel is compared to post-test PFA results using the COSTR damage model. For the compression load case, PFA results yield stiffer responses than the test panel by approximately 11%. The test data in Figure 11a is from the 2BC-C-1-1 panel. The main reason for this could be the out-of-plane constraint applied to the nodes in the finite element models, which significantly reduces the flexibility to a greater extent than in the experiment. Also, the models do not account for any geometric imperfection of the test panel, or non-uniform load application, which would also contribute to a stiffer response with the model. For the tension load case, the stiffness of COSTR finite element model and the test panel match very well. The test data in Figure 11b is of a 2BC-T-1-2 panel. The failure load obtained from COSTR damage model is lower likely because of not capturing the delamination damage mode. In general, when same direction plies are stacked together, the interface is prone to generate large inter-laminar shear stresses which causes delamination at the interface. The delamination will reduce the stress concentration and slow down the failure process. This is evident in the small failed tension panel pictures shown in Figure 4, in the form of wider damage zone consisting of fiber pull out, fiber breakage, and delaminations.

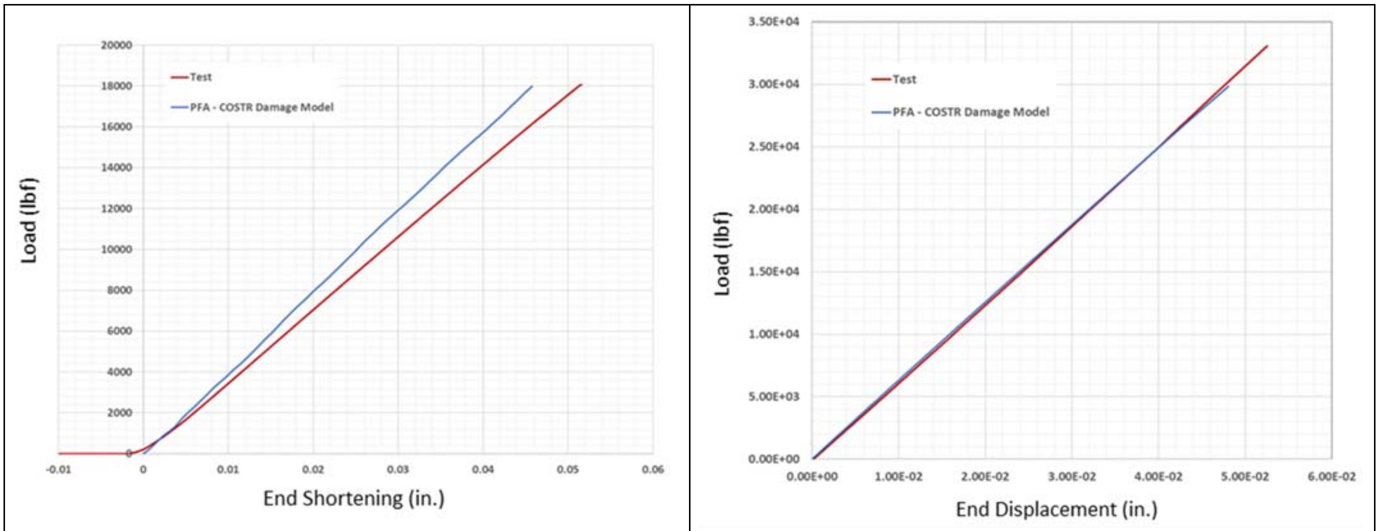


| a. Small Compression Panel | b. Small Tension Panel |
|---|---|

**Figure 11: Load versus End Displacement of Small Panels**

In Figure 12, the load versus end displacement response from an intermediate panel tested in compression and tension are compared to the post-test PFA results using the COSTR damage model. Excellent agreement is noticed in the stiffness with COSTR damage model and test panel for compression load case. The test data presented in Figure 12a for the compression load case is from panel 2BC-C-4-2. In the case of tension load, the stiffness from COSTR damage model matches well with the test panel. The test data presented in Figure 12b is of the panel 2BC-T-4-1.

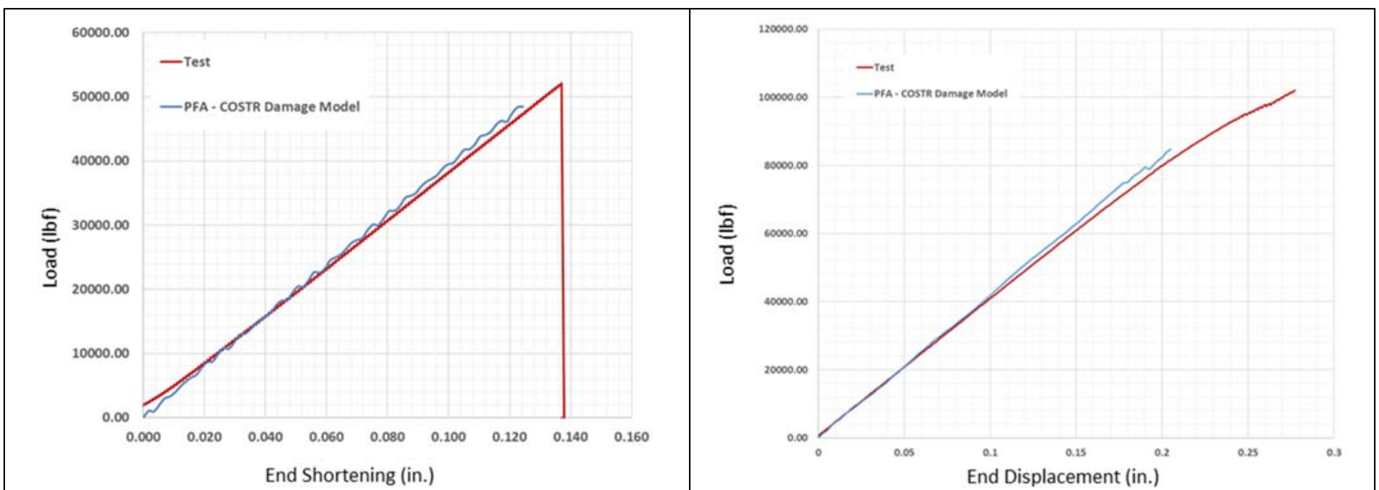


| a. Intermediate Compression Panel | b. Intermediate Tension Panel |
|---|---|

**Figure 12: Load versus End Displacement of Intermediate Panels**

## VI. Concluding Remarks

PFA of small and intermediate unstiffened notched composite laminate panels was performed in this study to aid in test planning and to evaluate the FEMs in comparison to the test data. PFA of the panels were performed using both COSTR and Abaqus built-in damage models to assess pre-test predictive capability of failure load and mode. Finite element models using shell elements were developed to perform PFA and hence the failure mode was limited to in-plane failure, such as fiber and matrix damages. Overall, the failure mode predicted from PFA was found to be in good agreement with the failed test panels, where all panels exhibited a self-similar failure mode initiated at the notch tip. Pre-test PFA predictions of failure load from both the models was found to correlate well for the compression panels tested where the differences were less than 12%. Larger discrepancies were observed when tension test results were compared to the pre-test PFA analyses with percent differences near 40% for the intermediate panels. Additional post-test analyses were performed where material properties were updated based on consideration of additional available material property data. For the post-test analyses, the failure load predictions by COSTR damage model improved and was found to be in better agreement with test data. The failure load predictions of the small panels were within -1 % and -12% for compression and tension load cases, respectively. For the intermediate panels, the COSTR predicted failure load was within -7.8% for the compression load and was within -23% for the tension load case. Similarly, the post-test failure load predictions by Abaqus built-in damage model of the small panels were within +2 % and -16% for compression and tension load cases, respectively. For the intermediate panels, the predicted failure load by Abaqus built-in damage model was within -12% for the compression load and was within -26% for the tension load case. Again, larger discrepancies were observed for the tension load cases than for the compression load cases which is likely due to the shell FEMs not capturing the delamination of the outer plies occurring during the tension tests.

Overall, the shell models used in the PFA analysis, along with considering the post-test analyses, are observed to be sufficient to obtain failure load within 15% for all panels tested in this study except the intermediate tension panel. The self-similar failure mode of the laminate that causes catastrophic failure can also be captured accurately with shell models. However to increase accuracy of failure load prediction, especially for the tension load cases where delaminations occurred, higher fidelity models need to be developed to simulate delamination at certain interfaces as was observed in both small and intermediate tested panels.

## Acknowledgements

The authors would like to thank William Avery from the Boeing Company for testing and providing the test data of the intermediate compression panels. The authors are also thankful for the Advanced Composites Program at NASA LaRC for providing funds and the opportunity to work on this task.

## References

[1]Enjuto, P., et al.," Investigation of Stiffening and Curvature Effects on the Residual Strength of Composite Stiffened Panels with Large Transverse Notches", Proceedings of the 2018 AIAA/ASME/ASCE/AHS/ASC Structures, Structural Dynamics and Materials Conference, Kissimmee, Florida, January 2018.

[2]Wanthal, S., et al., "Verification and Validation Process for Progressive Damage and Failure Analysis Methods in the NASA Advanced Composites Consortium", 32nd American Society for Composites Conference, West Lafayette, 2017.

[3]Mar, J.W. and K.Y.Lin., 1977,"Fracture Mechanics Correlation for Tensile Failure of Filamentary Composites with Holes," *J. of Aircraft*, 14(7):703:704.

[4]Dawn C. Jegley, Allen Waters, Jr., and Alana Zahn, "Testing of Composite Laminate Specimens with Mid-Length Lateral Notches", NASA/ TM-2020-5001774.

[5]Dassault Systems, 2013. "Damage and Failure for Fiber Reinforced Composites: Overview," in *ABAQUS Analysis User's Guide*, Version 6.13, Section 24.3.1.

[6]Satyanarayana, A., Bogert, P., Karayev, Z. K., Nordman, S. P., Hamid, "Influence of Finite Element Size in Residual Strength Prediction of Composite Structures," Proceedings of the 53rd AIAA/ASME/ASCE/AHS/ASC Structures, Structural Dynamics and Materials Conference, Honolulu, Hawaii, April 2012, AIAA-2012-1619.

[7]William Avery, "Test Results for Compression Loaded Flat Unstiffened Composite Laminates with Lateral Notches – 20x60 Coupons", Boeing Research and Technology, 5 February 2019, Seattle, WA.

[8]Hashin, Z., "Failure Criteria for Unidirectional Fiber Composites," *Journal of Applied Mechanics*, Vol.47, pp.329-334, 1980.

[9]Hashin, Z., and Rotem, A., "A Fatigue Failure Criteria for Fiber Reinforced Composite Materials," *Journal of Composite Materials*, Vol.7, pp.448-464, October 1973.

[10]Satyanarayana, A., and Bogert, B. P., "Influence of Shear Stiffness Degradation on Crack paths in Uni-directional Composite Laminates," NASA/TM-2017-219641.

[11]Hexel Corporation, "HexPly 8552 Product Data sheet". https://www.hexcel.com/user_area/content_media/raw/HexPly_8552_us_DataSheet.pdf

[12]Kristin Marlett, NIAR, "Hexcel 8552 IM7 Unidirectional Prepreg 190 gsm & 35%RC Qualification Material Property Data Report", NCAMP Test Report: CAM-RP-2009-015 Rev A, Page 33, April 22, 2011.

[13]Bazant, Z. P., and Oh, B. H., "Crack band theory for fracture of concrete", *Materials and structures*, vol 16, PP 155-177, 1983

# APPENDIX

Material Data Sheet of IM7/8552-1 – from NCAMP report

| | | | | |
|---|---|---|---|---|
| **Prepreg Material:** | Hexcel Corporation - Hexcel 8552 IM7 Unidirectional<br>NMS 128/2 Material Specification | | | **Hexcel 8552 IM7<br>Unidirectional Tape<br>Lamina Properties Summary** |
| **Fiber** | IM7 unidirectional | **Resin** | Hexcel 8552 | |
| **Tg(dry)** | 406.43 °F | **Tg(wet)** | 321.41 °F | |
| **PROCESSING:** | NPS 81228 "M" Cure Cycle | | **Tg METHOD** DMA (SRM 18-94) | |

| | Lot 1 | Lot 2 | Lot 3 | | |
|---|---|---|---|---|---|
| **Date of fiber manufacture** | 01/26/2007 | 12/25/2006 | 02/05/2007 | **Date of testing** | 1/22/2008 - 3/4/10 |
| **Date of resin manufacture** | 02/28/2007 | 01/24/2007 | 03/01/2007 | **Date of data submittal** | 4/5/2010 |
| **Date of prepreg manufacture** | 02/28/2007 | 01/24/2007 | 03/01/2007 | | |
| **Date of composite manufacture** | 9/2007 to 10/2007 | | | | |

**LAMINA MECHANICAL PROPERTY SUMMARY**
**Data reported as: Normalized & Measured**
**(Normalized by CPT = 0.0072 inch)**

| | CTD Mean | | RTD Mean | | ETD Mean | | ETW Mean | |
|---|---|---|---|---|---|---|---|---|
| | Normalized | Measured | Normalized | Measured | Normalized | Measured | Normalized | Measured |
| $F_1^{tu}$ (ksi) from LT | 357.39 | 353.70 | 362.69 | 371.08 | --- | --- | 333.50 | 327.96 |
| $F_1^{tu}$ (ksi) from UNT0 | 286.78 | 281.57 | 324.62 | 320.79 | --- | --- | 346.85 | 340.46 |
| $E_1^t$ (Msi) of LT | 22.57 | 22.33 | 22.99 | 23.51 | --- | --- | 24.00 | 23.77 |
| E (Msi) of UNT0 | 11.92 | 11.71 | 11.99 | 11.85 | --- | --- | 11.94 | 11.74 |
| $\nu_{12}^t$ | | 0.270 | | 0.316 | | | | 0.393 |
| $F_2^{tu}$ (ksi) | --- | 9.60 | --- | 9.29 | --- | --- | --- | 3.49 |
| $E_2^t$ (Msi) of TT | --- | 1.46 | --- | 1.30 | --- | --- | --- | 0.81 |
| $F_1^{cu}$ (ksi) from UNC0 | 296.49 | 291.99 | 248.94 | 251.13 | 201.93 | 199.50 | 173.00 | 172.58 |
| $E_1^c$ (Msi) of LC | 20.68 | 20.53 | 20.04 | 20.44 | 20.25 | 20.00 | 20.37 | 20.65 |
| E (Msi) of UNC0 | 7.75 | 7.64 | 7.47 | 7.52 | 7.57 | 7.53 | 7.74 | 7.82 |
| $\nu_{12}^c$ | --- | 0.362 | | 0.356 | | 0.374 | | 0.383 |
| $F_2^{cu}$ (ksi) of TC | --- | 55.31 | --- | 41.44 | --- | --- | --- | 19.02 |
| $E_2^c$ (Msi) of TC | --- | 1.53 | --- | 1.41 | --- | --- | --- | 1.18 |
| $\nu_{21}^c$ of TC | --- | 0.028 | --- | 0.024 | --- | --- | --- | 0.018 |
| $\nu$ of UNC0 | --- | 0.041 | | 0.035 | | 0.030 | | 0.017 |
| $F_{12}^{s5\%strain}$ (ksi) | --- | --- | --- | 13.22 | --- | --- | --- | 5.54 |
| $F_{12}^{s0.2\%}$ (ksi) | --- | 11.29 | --- | 7.76 | --- | --- | --- | 3.31 |
| $G_{12}^s$ (Msi) | --- | 0.86 | --- | 0.68 | --- | --- | --- | 0.31 |
| SBS (ksi) | --- | 21.04 | --- | 17.13 | --- | 11.23 | --- | 8.25 |

* Derived from cross-ply using back-out factor

Material Data Sheet of IM7/8552-1 – Hexcel Product Data Sheet.

# HexPly® 8552

Mid-Toughened, High Strength, Damage-Resistant, Structural Epoxy Matrix

HEXCEL

Product Data Sheet

## Mechanical Properties

| Property | Temp°F | Condition | AS4 | IM7 | A193-PW | A280-5H | SGP196-PW | SGP370-8H | S2GL |
|---|---|---|---|---|---|---|---|---|---|
| 0° Tensile strength, ksi | -67 | Dry | 300 | 373 | 111 | 120 | 142 | 140 | - |
| 0° Tensile modulus, msi | -67 | Dry | 19.4 | 23.7 | 9.5 | 10.2 | 12.3 | 12.5 | - |
| 0° Tensile strength, ksi | 77 | Dry | 310 | 395 | 120 | 127 | 158 | 147 | 251 |
| 0° Tensile modulus, msi | 77 | Dry | 19.6 | 23.8 | 9.8 | 9.7 | 12.3 | 12.4 | 6.53 |
| 0° Tensile elongation, % | 77 | Dry | 1.55 | 1.62 | - | - | - | - | 3.87 |
| 0° Tensile strength, ksi | 195 | Dry | 293 | **368*** | 116 | 131 | - | - | - |
| 0° Tensile modulus, msi | 195 | Dry | 19.1 | **23.7*** | 9.6 | 10 | - | - | - |
| 90° Tensile strength, ksi | -67 | Dry | 9.73 | 9.60 | 103 | 109 | 125 | 131 | - |
| 90° Tensile modulus, msi | -67 | Dry | 1.50 | 1.46 | 9.6 | 9.7 | 11.6 | 11.7 | - |
| 90° Tensile strength, ksi | 77 | Dry | 9.27 | 9.3 | 115 | 116 | 137 | 139 | - |
| 90° Tensile modulus, msi | 77 | Dry | 1.39 | 1.70 | 9.5 | 9.5 | 11.6 | 11.7 | - |
| 90° Tensile strength, ksi | 200 | Dry | - | - | 111 | 112 | **142*** | **130*** | - |
| 90° Tensile modulus, msi | 200 | Dry | 1.22 | 1.50 | 9.8 | 9.4 | **11.5*** | **11.5*** | - |
| Major Poisson's Ratio, tension | 77 | Dry | 0.302 | 0.316 | - | - | - | - | - |
| ± 45 Inplane shear | 77 | Dry | 16.6 | 17.4 | - | 15.9 | 18.3 | 1436 | - |
| ± 45 Inplane shear | 200 | Dry | 15.2 | **15.4*** | - | - | **15.5*** | **13.1*** | - |
| Major Poisson's Ratio, compression | 77 | Dry | 0.335 | 0.356 | - | - | - | - | - |
| 0° Compression strength, ksi | -67 | Dry | 253 | 292 | 139 | - | - | - | - |
| 0° Compression modulus, msi | -67 | Dry | 18 | 20.5 | 8.7 | - | - | - | - |
| 0° Compression strength, ksi | 77 | Dry | 222 | 245 | 128 | 134 | - | - | 217 |

## REPORT DOCUMENTATION PAGE

*Form Approved*
*OMB No. 0704-0188*



**1. REPORT DATE** *(DD-MM-YYYY)*
01-06-2020

**2. REPORT TYPE**
Technical Memorandum

**3. DATES COVERED** *(From - To)*

**4. TITLE AND SUBTITLE**
Progressive Failure Analysis Correlation with Notched Composite Laminate Test Data

**5a. CONTRACT NUMBER**

**5b. GRANT NUMBER**

**5c. PROGRAM ELEMENT NUMBER**

**6. AUTHOR(S)**
Arunkumar, Satyanarayar; Walker, Sandra P.; Gould, Kevin E.

**5d. PROJECT NUMBER**

**5e. TASK NUMBER**

**5f. WORK UNIT NUMBER**
081876.01.07.05

**7. PERFORMING ORGANIZATION NAME(S) AND ADDRESS(ES)**
NASA Langley Research Center
Hampton, VA 23681-2199

**8. PERFORMING ORGANIZATION REPORT NUMBER**

**9. SPONSORING/MONITORING AGENCY NAME(S) AND ADDRESS(ES)**
National Aeronautics and Space Administration
Washington, DC 20546-0001

**10. SPONSOR/MONITOR'S ACRONYM(S)**
NASA

**11. SPONSOR/MONITOR'S REPORT NUMBER(S)**
NASA-TM-2020-5003145

**12. DISTRIBUTION/AVAILABILITY STATEMENT**
Unclassified
Subject Category : Composite Materials
Availability: NASA STI Program (757) 864-9658

**13. SUPPLEMENTARY NOTES**

**14. ABSTRACT**
Testing of small and intermediate laminate panels with notches was performed and Progressive Failure Analyses (PFA) models were developed for aid in test planning and for correlation with the test data. Two progressive damage failure models were included in the study: the commercially available Abaqus built-in damage model and COmplete STress Reduction (COSTR) damage model developed at NASA Langley Research Center (LaRC). The finite elements models used for the analysis were developed using shell elements. The pre-test PFA results obtained from the two damage models were compared to test data. Then a post-test PFA with updated material properties based on additional available material property data was executed with the COSTR damage model and compared to the test data. The panels tested in compression all exhibited less scatter in the failure load with self-similar failure behavior. The panels tested in tension exhibited more scatter in the failure load with a failure mode that included delamination of plies.

**15. SUBJECT TERMS**
Damage Model; Progressive Failure Analysis; Open Hole Tension; Open Hole Compression

| 16. SECURITY CLASSIFICATION OF: a. REPORT | b. ABSTRACT | c. THIS PAGE | 17. LIMITATION OF ABSTRACT | 18. NUMBER OF PAGES | 19a. NAME OF RESPONSIBLE PERSON |
|---|---|---|---|---|---|
| U | U | U | UU | 25 | STI Help Desk (email: help@sti.nasa.gov) |
| | | | | | **19b. TELEPHONE NUMBER** *(Include area code)* (757) 864-9658 |

**Standard Form 298** (Rev. 8/98)
Prescribed by ANSI Std. Z39.18